JOURNAL OF THEORETICAL AND APPLIED MECHANICS
62, 1, pp. 3-17, Warsaw 2024
https://doi.org/10.15632/jtam-pl/174698

BENDING OF A SANDWICH BEAM WITH AN INDIVIDUAL FUNCTIONALLY GRADED CORE

Krzysztof Magnucki
Łukasiewicz Research Network – Poznan Institute of Technology, Rail Vehicles Center Poznan, Poland
e-mail: krzysztof.magnucki@pit.lukasiewicz.gov.pl

Krzysztof Sowiński
Poznan University of Technology, Institute of Applied Mechanics, Poznan, Poland
e-mail: krzysztof.sowinski@put.poznan.pl

This paper is devoted to a clamped sandwich beam with an individual functionally graded core under a uniformly distributed load. A non-linear shear deformation theory is developed with consideration of the classical shear stress formula for beams. Two differential equations of the equilibrium of the beam are obtained based on the principle of stationary total potential energy. The shear effect function and the relative deflection line of the beam are determined. Moreover, a numerical FEM model (Ansys system) of this beam is elaborated. Detailed calculations of exemplary beams are realised using two methods, analytical and numerical FEM.

Keywords: sandwich beam, functionally graded core, non-linear shear deformation theory

1. Introduction

Shear deformation theories of beams, plates and shells have been extensively refined in the twenty-first century. The demand for new, more accurate and generalised shear theories becomes more apparent with increasing interest in the application of composite structures in engineering. The significance of this topic can be proven by the number of articles and original theories developed over the last two decades.

Huang (2003) described various studies on stress-strain modelling of adhesively bonded sandwich beams and proposed his model of sandwich beams. Reddy (2004) presented a fundamental theory and analysis associated with the mechanics of laminated composite plates and shells. Zenkour (2006) modelled a static response for a rectangular plate supported with a functionally graded plate.

Berdichevsky (2010) derived a two-dimensional theory of sandwich plates by asymptotic analysis of three-dimensional linear elasticity. Carrera *et al.* (2011) discussed classical and modern approaches to the beam theory and paid particular attention to their typical applications. Meiche *et al.* (2011) developed an advanced hyperbolic shear deformation theory. Mantari *et al.* (2012) presented an original shear deformation theory for sandwich and composite plates, where the displacement field is parameterized. Thai and Vo (2013) proposed a sinusoidal shear deformation theory for bending, buckling and vibration of functionally graded plates. Sahoo and Singh (2013) discussed an original inverse trigonometric zigzag theory and implemented it for static analysis of laminated composite and sandwich panels.

Kolakowski and Mania (2015) investigated the dynamic interactive response of square FGM plates subjected to in-plane pulse loading using the modified classical laminate plate theory. Mahi *et al.* (2015) introduced a hyperbolic shear deformation theory with five degrees of freedom applicable to bending and free vibration analysis of isotropic, functionally graded sandwich and

laminated composite plates. Marczak and Jędrysiak (2015) studied free-vibration of periodic three-layered sandwich structures referring to Kirchoff's thin plate theory and the tolerance averaging technique. Domagalski and Jędrysiak (2016) presented a work on geometrically non-linear vibrations of beams with periodic structures.

Banat and Mania (2017) considered non-linear buckling and failure analysis of fibre metal laminate thin-walled structures under axial compression. Özütok and Madenci (2017) presented a higher-order shear deformation theory including a non-linear distribution of shear stress through the thickness of a laminated beam. Pei *et al.* (2018) established a variationally consistent higher-order theory for problems of functionally graded beams, referring to the principle of virtual work. Birman and Kardomateas (2018) discussed the current development and interest in mathematical modelling and the application of sandwich structures. Ghayesh (2018) focused on vibrations of axially functionally graded beams incorporating shear deformation and imperfection.

Kumar *et al.* (2019) developed a modern higher-order shear deformation theory for a functionally graded plate. Magnucki *et al.* (2020) referred to the Zhuravsky shear stress formula to develop a shear deformation theory. Żur *et al.* (2020) focused on buckling and free-vibration analyses of functionally graded nanoplates with magneto-electroelastic coupling. Dhuria *et al.* (2021) analysed the effect of porosity distribution on the static and buckling response of a simply supported plate with FGM.

Magnucki (2022) presented analytical models of homogeneous beams with bi-symmetrical cross sections, sandwich beams and beams with symmetrically varying mechanical properties. Magnucki *et al.* (2022) conducted a study on the axisymmetric bending problem of a generalised circular sandwich plate with varying mechanical properties along its thickness. Jędrysiak (2023) investigated slender, elastic, nonperiodic beams with a functionally graded structure on the macro-level and a nonperiodic structure on the micro-level referring to the tolerance modelling method.

The main objective of the study is to formulate a linear theory with the assumption of a non-linear shear deformation for a three-layer beam with an individual functionally graded core. The function of the variation of Young's modulus is generalised so that it can describe a beam with homogeneous mechanical properties, as well as a classic three-layer and five-layer beam with an optional ratio of stiffness between the layers.

According to the literature review, there are numerous papers investigating the problem of the shear effect in structures. Many of them refer to a numerical approach or analytical formulation with a predefined, usually parametric shear deformation function. In the present paper, the shear deformation function is obtained analytically in the exact manner with consideration of the classical shear stress formula. An analytical model of a beam is developed using the proposed non-linear shear deformation theory. The subject of the study is a clamped sandwich beam of length L, width b, and total depth h with an individual functionally graded core under a uniformly distributed load of intensity q (Fig. 1). The bending problem of this beam is studied, taking into account the shear effect. Its solution is compared with the results of numerical finite element method analysis in the Ansys system.

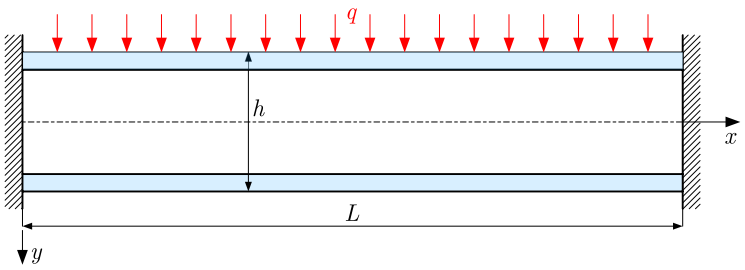

Fig. 1. A scheme of a clamped sandwich beam with an individual functionally graded core

2. Analytical model of the sandwich beam

The rectangular cross section and variation of Young's modulus in the depth direction of the beam are shown in Fig. 2.

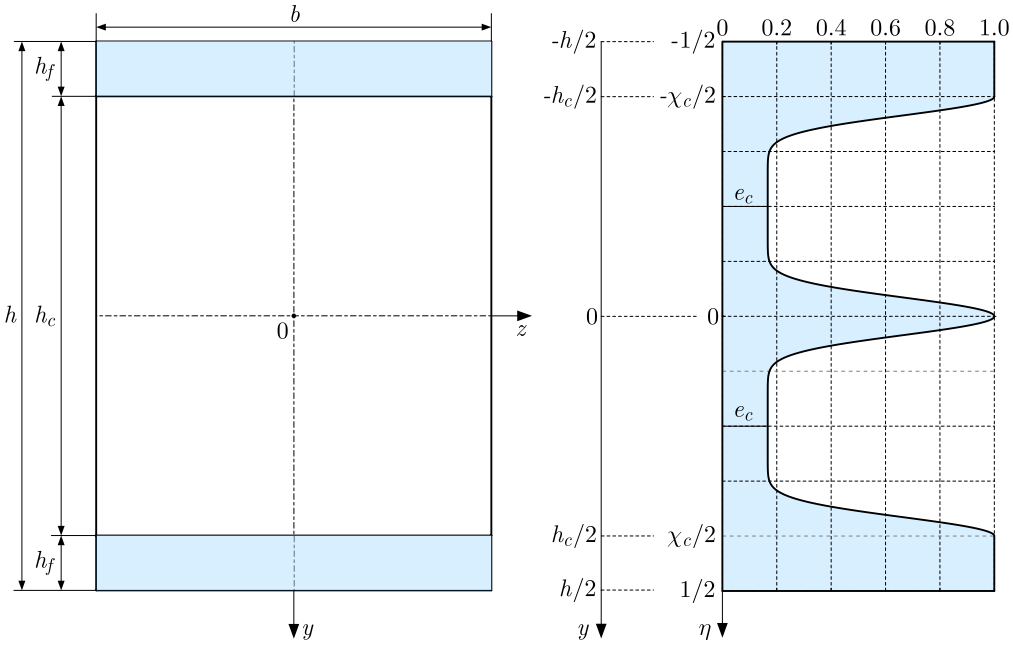

Fig. 2. Schemes of the rectangular cross section and variation of Young's modulus in the depth direction of the beam

The variation of Young's modulus in the depth direction takes the form

$$E_f(\eta) = E_f f_e(\eta) \tag{2.1}$$

where: E_f – Young's modulus of faces, also $f_e(\eta)$ – dimensionless function, which in successive layers is as follows:
— the upper face $(-1/2 \leqslant \eta \leqslant -\chi_c/2)$

$$f_e(\eta) = 1 \tag{2.2}$$

— the core $(-\chi_c/2 \leqslant \eta \leqslant \chi_c/2)$

$$f_e(\eta) = e_c + \frac{1-e_c}{2^n}\Big[1+\cos\Big(\frac{4}{\chi_c}\pi\eta\Big)\Big]^n \tag{2.3}$$

— the lower face $(\chi_c/2 \leqslant \eta \leqslant 1/2)$

$$f_e(\eta) = 1 \tag{2.4}$$

and dimensionless quantities: the coordinate $\eta = y/h$, coefficient of the core e_c, thickness of the core $\chi_c = h_c/h$, exponent n – natural number. The deformation of a planar cross section after bending of this beam is presented in Fig. 3. The longitudinal displacements according to this scheme (Fig. 3) in successive layers are as follows:
— the upper face $(-1/2 \leqslant \eta \leqslant -\chi_c/2)$

$$u^{(uf)}(x,\eta) = -h\Big[\eta\frac{dv}{dx} - f_d^{(uf)}(\eta)\psi_f(x)\Big] \tag{2.5}$$

— the core $(-\chi_c/2 \leqslant \eta \leqslant \chi_c/2)$

$$u^{(c)}(x,\eta) = -h\Big[\eta\frac{dv}{dx} - f_d^{(c)}(\eta)\psi_f(x)\Big] \tag{2.6}$$

— the lower face $(\chi_c/2 \leqslant \eta \leqslant 1/2)$

$$u^{(lf)}(x,\eta) = -h\Big[\eta\frac{dv}{dx} - f_d^{(lf)}(\eta)\psi_f(x)\Big] \tag{2.7}$$

where: $v(x)$ – deflection, $\psi_f(x) = u_f(x)/h$ – dimensionless longitudinal displacement on the outer surfaces of the beam-shear effect function, $f_d^{(uf)}(\eta)$, $f_d^{(c)}(\eta)$, $f_d^{(lf)}(\eta)$ – dimensionless deformation functions in these layers.

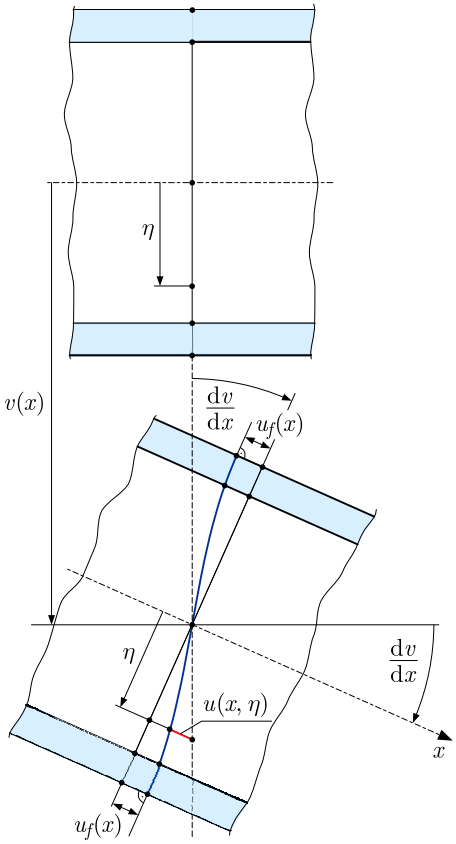

Fig. 3. Scheme of a planar cross-section deformation of the analysed beam

Consequently, the strains and stresses are as follows:
— the upper face $(-1/2 \leqslant \eta \leqslant -\chi_c/2)$

$$\begin{aligned}
\varepsilon_x^{(uf)}(x,\eta) &= \frac{\partial u}{\partial x} = -h\Big[\eta\frac{d^2v}{dx^2} - f_d^{(uf)}(\eta)\frac{d\psi_f}{dx}\Big] \\
\sigma_x^{(uf)}(x,\eta) &= -E_f h\Big[\eta\frac{d^2v}{dx^2} - f_d^{(uf)}(\eta)\frac{d\psi_f}{dx}\Big] \\
\gamma_{xy}^{(uf)}(x,\eta) &= \frac{dv}{dx} + \frac{\partial u}{h\partial\eta} = \frac{df_d^{(uf)}}{d\eta}\psi_f(x) \\
\tau_{xy}^{(uf)}(x,\eta) &= \frac{E_f}{2(1+\nu)}\frac{df_d^{(uf)}}{d\eta}\psi_f(x)
\end{aligned} \tag{2.8}$$

— the core $(-\chi_c/2 \leqslant \eta \leqslant \chi_c/2)$

$$\begin{aligned}
\varepsilon_x^{(c)}(x,\eta) &= \frac{\partial u}{\partial x} = -h\Big[\eta\frac{d^2v}{dx^2} - f_d^{(c)}(\eta)\frac{d\psi_f}{dx}\Big] \\
\gamma_{xy}^{(c)}(x,\eta) &= \frac{dv}{dx} + \frac{\partial u}{h\partial\eta} = \frac{df_d^{(c)}}{d\eta}\psi_f(x) \\
\sigma_x^{(c)}(x,\eta) &= -E_f h\Big[\eta\frac{d^2v}{dx^2} - f_d^{(c)}(\eta)\frac{d\psi_f}{dx}\Big] f_e^{(c)}(\eta) \\
\tau_{xy}^{(c)}(x,\eta) &= \frac{E_f}{2(1+\nu)} f_e^{(c)}(\eta)\frac{df_d^{(c)}}{d\eta}\psi_f(x)
\end{aligned} \tag{2.9}$$

— the lower face $(\chi_c/2 \leqslant \eta \leqslant 1/2)$

$$\begin{aligned}
\varepsilon_x^{(lf)}(x,\eta) &= \frac{\partial u}{\partial x} = -h\Big[\eta\frac{d^2v}{dx^2} - f_d^{(lf)}(\eta)\frac{d\psi_f}{dx}\Big] \\
\gamma_{xy}^{(lf)}(x,\eta) &= \frac{dv}{dx} + \frac{\partial u}{h\partial\eta} = \frac{df_d^{(lf)}}{d\eta}\psi_f(x) \\
\sigma_x^{(lf)}(x,\eta) &= -E_f h\Big[\eta\frac{d^2v}{dx^2} - f_d^{(lf)}(\eta)\frac{d\psi_f}{dx}\Big] \\
\tau_{xy}^{(lf)}(x,\eta) &= \frac{E_f}{2(1+\nu)}\frac{df_d^{(lf)}}{d\eta}\psi_f(x)
\end{aligned} \tag{2.10}$$

where ν – Poisson's ratio is constant for the structure. Taking into account the papers by Magnucki (2022) and Magnucki *et al.* (2022), the unknown dimensionless deformation functions $f_d^{(uf)}(\eta)$, $f_d^{(c)}(\eta)$, $f_d^{(lf)}(\eta)$ are determined with consideration of the classical shear stress formula for the rectangular cross section of the beam

$$\tau_{xy}^{(Cl)}(x,\eta) = \overline{Q}_z(\eta)\frac{T(x)}{J_z}h^2 \tag{2.11}$$

where: $T(x)$ – transverse-shear force, $\overline{Q}_z(\eta)$ – dimensionless first moment of the cross section area part, J_z – inertia moment of the cross section. Therefore, the dimensionless first moments of successive layers of this sandwich beam with the individual functionally graded core are of the form:

— the upper face $(-1/2 \leqslant \eta \leqslant -\chi_c/2)$

$$\overline{Q}_z^{(uf)}(\eta) = \frac{1}{8}(1-4\eta^2) \tag{2.12}$$

— the core $(-\chi_c/2 \leqslant \eta \leqslant \chi_c/2)$

$$\overline{Q}_z^{(c)}(\eta) = \frac{1}{8}[1-\chi_c^2 + e_c(\chi_c^2 - 4\eta^2) - 8J_c(\eta)] \tag{2.13}$$

where

$$J_c(\eta) = \frac{1-e_c}{2^n}\int\limits_{-\chi_c/2}^{\eta}\Big(1+\cos\frac{4\pi\eta_1}{\chi_c}\Big)^n\eta_1\,d\eta_1 \tag{2.14}$$

— the lower face $(\chi_c/2 \leqslant \eta \leqslant 1/2)$

$$\overline{Q}_z^{(lf)}(\eta) = \frac{1}{8}(1-4\eta^2) \tag{2.15}$$

Equating the shear stresses in Eqs. (2.8), (2.9) and (2.10) with classical shear stress formula (2.11) with consideration of the dimensionless first moments in Eqs. (2.12), (2.13) and (2.14), after simple transformations, the unknown dimensionless deformation functions for successive layers satisfying the continuity conditions between them are obtained in the following form:
— the upper face $(-1/2 \leqslant \eta \leqslant -\chi_c/2)$

$$f_d^{(uf)}(\eta) = -C_f + \frac{1}{24}(3 - 4\eta^2)\eta \tag{2.16}$$

— the core $(-\chi_c/2 \leqslant \eta \leqslant \chi_c/2)$

$$f_d^{(c)}(\eta) = \int \frac{\overline{Q}_z^{(c)}(\eta)}{f_e(\eta)}\, d\eta \tag{2.17}$$

— the lower face $(\chi_c/2 \leqslant \eta \leqslant 1/2)$

$$f_d^{(uf)}(\eta) = C_f + \frac{1}{24}(3 - 4\eta^2)\eta \tag{2.18}$$

where the dimensionless coefficient

$$C_f = -\frac{1}{48}(3 - \chi_c^2)\chi_c + \int_0^{\chi_c/2} \frac{\overline{Q}_z^{(c)}(\eta)}{f_e(\eta)}\, d\eta \tag{2.19}$$

The graph of dimensionless functions in Eqs. (2.2), (2.3) and (2.4) of the variation of Young's modulus and the shape of deformation of the planar cross section of an exemplary beam ($\chi_c = 4/5$, $e_c = 1/30$, $n = 7$), taking into account functions Eqs. (2.16), (2.17) and (2.8), is shown in Fig. 4.

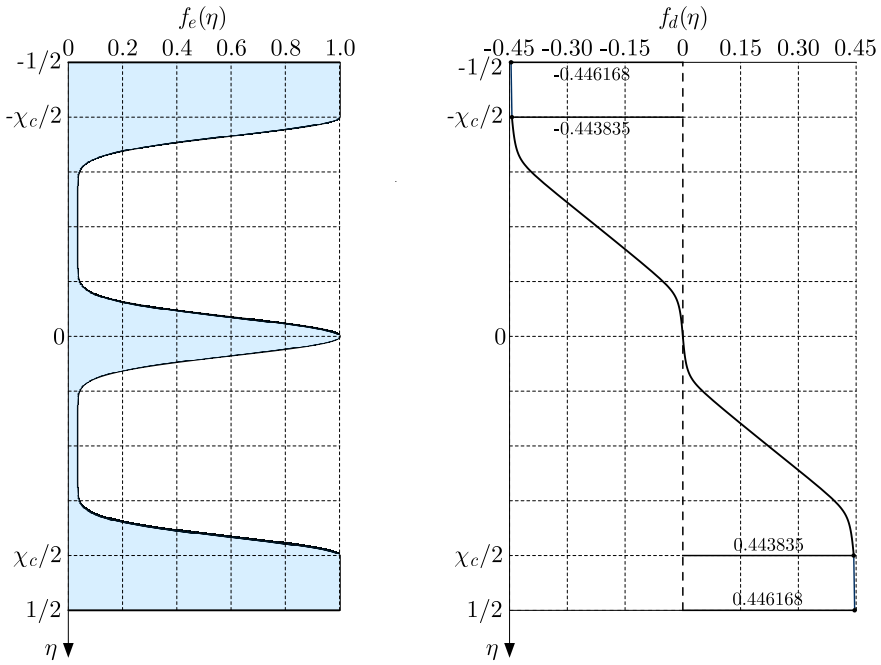

Fig. 4. The graph of dimensionless functions of Young's modulus variation and the shape of deformation of the planar cross section of the exemplary beam

3. Analytical bending study of the sandwich beam

The elastic strain energy is described as

$$U_e = \frac{1}{2} E_f b h \int_0^L \Big[\Phi_{\varepsilon,\gamma}^{(uf)}(x) + \Phi_{\varepsilon,\gamma}^{(c)}(x) + \Phi_{\varepsilon,\gamma}^{(lf)}(x) \Big] \, dx \tag{3.1}$$

where

$$\Phi_{\varepsilon,\gamma}^{(uf)}(x) = \int_{-1/2}^{-\chi_c/2} \Big\{ \big[\varepsilon_x^{(uf)}(x,\eta)\big]^2 + \frac{1}{2(1+\nu)} \big[\gamma_{xy}^{(uf)}(x,\eta)\big]^2 \Big\} \, d\eta$$

$$\Phi_{\varepsilon,\gamma}^{(c)}(x) = \int_{-\chi_c/2}^{\chi_c/2} \Big\{ \big[\varepsilon_x^{(c)}(x,\eta)\big]^2 + \frac{1}{2(1+\nu)} \big[\gamma_{xy}^{(c)}(x,\eta)\big]^2 \Big\} f_e(\eta) \, d\eta$$

$$\Phi_{\varepsilon,\gamma}^{(lf)}(x) = \int_{\chi_c/2}^{1/2} \Big\{ \big[\varepsilon_x^{(lf)}(x,\eta)\big]^2 + \frac{1}{2(1+\nu)} \big[\gamma_{xy}^{(lf)}(x,\eta)\big]^2 \Big\} \, d\eta$$

Substituting expressions in Eqs. $(2.8)_{1,3}$, $(2.9)_{1,2}$, $(2.10)_{1,2}$ for strains into Eq. (3.1), after integration, one obtains

$$U_e = \frac{1}{24} E_f b h^3 \int_0^L \Big[C_{vv} \Big(\frac{d^2 v}{dx^2}\Big)^2 - 2 C_{v\psi} \frac{d^2 v}{dx^2} \frac{d\psi_f}{dx} + C_{\psi\psi} \Big(\frac{d\psi_f}{dx}\Big)^2 + C_\psi \frac{\psi_f(x)^2}{h^2} \Big] \, dx \tag{3.2}$$

where the dimensionless coefficients

$$C_{vv} = 1 - \chi_c^3 + 12 J_{vv} \qquad C_{v\psi} = 3(1-\chi_c^2) C_f + \frac{1}{40}(4 - 5\chi_c^3 + \chi_c^5) + 12 J_{v\psi}$$

$$C_{\psi\psi} = \frac{1}{672} \Big\{ 84[96(1-\chi_c) C_f + 5 - 6\chi_c^2 + \chi_c^4] C_f + \frac{1}{10}(68 - 105\chi_c^3 + 42\chi_c^5 - 5\chi_c^7) \Big\} + 12 J_{\psi\psi}$$

$$C_\psi = \frac{1}{2(1+\nu)} \Big[\frac{1}{80}(8 - 15\chi_c + 10\chi_c^3 - 3\chi_c^5) + 12 J_\psi \Big]$$

$$J_{vv} = \int_{-\chi_c/2}^{\chi_c/2} \eta^2 f_e(\eta) \, d\eta \qquad J_{v\psi} = \int_{-\chi_c/2}^{\chi_c/2} \eta f_d^{(c)}(\eta) f_e(\eta) \, d\eta$$

$$J_{\psi\psi} = \int_{-\chi_c/2}^{\chi_c/2} [f_d^{(c)}(\eta)]^2 f_e(\eta) \, d\eta \qquad J_\psi = \int_{-\chi_c/2}^{\chi_c/2} \Big(\frac{df_d^{(c)}}{d\eta}\Big)^2 f_e(\eta) \, d\eta$$

The work of the load is in the form

$$W = \int_0^L q v(x) \, dx \tag{3.3}$$

Based on the principle of stationary total potential energy $\delta(U_e - W) = 0$, the system of two differential equations of equilibrium of this sandwich beam is obtained in the following form

$$C_{vv} \frac{d^4 v}{dx^4} - C_{v\psi} \frac{d^3 \psi_f}{dx^3} = \frac{q}{E_f b h^3} \qquad C_{v\psi} \frac{d^3 v}{dx^3} - C_{\psi\psi} \frac{d^2 \psi_f}{dx^2} + C_\psi \frac{\psi_f(x)}{h^2} = 0 \tag{3.4}$$

The fourth-order expression, Eq. $(3.4)_1$, of this system is equivalent to the second-order equation of the form

$$C_{vv}\frac{d^2v}{dx^2} - C_{v\psi}\frac{d\psi_f}{dx} = -\frac{M_b(x)}{E_f b h^3} \tag{3.5}$$

where $M_b(x)$ is the bending moment. Thus, Eqs. (3.5) and $(3.4)_2$ are the governing equations of the sandwich beam. These two equations, after a simple transformation, are reduced to one equation in the form

$$\frac{d^2\psi_f}{d\xi^2} - (\alpha\lambda)^2\psi_f(\xi) = -\frac{C_{v\psi}}{C_{vv}C_{\psi\psi} - C_{v\psi}^2}\lambda^2\frac{T(\xi)}{E_f b h} \tag{3.6}$$

where: $\xi = x/L$ – dimensionless coordinate, $\lambda = L/h$ – relative length of the beam, and

$$\alpha = \sqrt{\frac{C_{vv}C_{\psi}}{C_{vv}C_{\psi\psi} - C_{v\psi}^2}}$$

is a dimensionless coefficient. The end part of this beam with a uniformly distributed load and reactions is shown in Fig. 5.

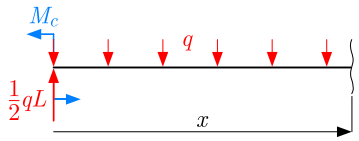

Fig. 5. Scheme of the beam end part with the load end reactions

The bending moment and the shear force according to this scheme, in the dimensionless coordinate ξ, are as follows

$$M_b(\xi) = \frac{1}{2}(\xi - \xi^2 - 2\overline{M}_c)qL^2 \qquad T(\xi) = \frac{1}{2}(1-2\xi)qL \tag{3.7}$$

where $\overline{M}_c = M_c/(qL^2)$ is the unknown dimensionless reactive moment. Therefore, Eq. (3.6), taking into account the transverse shear force in Eq. $(3.7)_2$, is of the form

$$\frac{d^2\psi_f}{d\xi^2} - (\alpha\lambda)^2\psi_f(\xi) = -6\frac{C_{v\psi}}{C_{vv}C_{\psi\psi} - C_{v\psi}^2}\lambda^3(1-2\xi^2)\frac{q}{E_f b} \tag{3.8}$$

The solution of this equation is as follows

$$\psi_f(\xi) = [C_1\sinh(\alpha\lambda\xi) + C_2\cosh(\alpha\lambda\xi) + C_0(1-2\xi)]\frac{q}{E_f b} \tag{3.9}$$

where C_1, C_2 are integration constants, and

$$C_0 = 6\frac{C_{v\psi}}{C_{vv}C_{\psi}}\lambda$$

Taking into account the two conditions: $\psi_f(0) = 0$ – clamped end, and $\psi_f(1/2) = 0$ – the symmetry plane of the beam, these constants are as follows $C_1 = C_0/\tanh(\alpha\lambda/2)$ and $C_2 = -C_0$. Consequently, the function in Eq. (3.9), that is, the shear effect function is in the following form

$$\psi_f(\xi) = \overline{\psi}_f(\xi)\frac{q}{E_f b} \tag{3.10}$$

where

$$\overline{\psi}_f(\xi) = 6\Big\{1 - 2\xi - \frac{\sinh[\alpha\lambda(1-2\xi)/2]}{\sinh(\alpha\lambda)/2}\Big\}\frac{C_{v\psi}}{C_{vv}C_\psi}\lambda \tag{3.11}$$

Equation (3.5) in the dimensionless coordinate, with consideration of the expressions in Eqs. (3.7) and (3.10), is as follows

$$\frac{d^2\overline{v}}{d\xi^2} = \Big[\frac{C_{v\psi}}{\lambda^3}\frac{d\overline{\psi}_f}{d\xi} - 6(\xi - \xi^2 - 2\overline{M}_c)\Big]\frac{\lambda^3}{C_{vv}}\frac{q}{E_f b} \tag{3.12}$$

where $\overline{v}(\xi) = v(\xi)/L$ is the relative deflection of the beam. Integrating this equation and taking into account the boundary condition $d\overline{v}/d\xi\big|_0 = 0$ – clamped end, and $d\overline{v}/d\xi\big|_{1/2} = 0$ – symmetry plane of the beam, one obtains

$$\frac{d\overline{v}}{d\xi} = \Big[\frac{C_{v\psi}}{\lambda^3}\overline{\psi}_f(\xi) - 6\Big(\frac{1}{2}\xi^2 - \frac{1}{3}\xi^3 - 2\overline{M}_c\xi\Big)\Big]\frac{\lambda^3}{C_{vv}}\frac{q}{E_f b} \tag{3.13}$$

where: $\overline{M}_c = 1/12$. Thus, integrating this equation and taking into account the boundary condition $\overline{v}(0) = 0$ and the function in Eq. (3.11), one obtains the relative deflection-bending line of the beam

$$\overline{v}(\xi) = \overline{v}(\xi)\frac{q}{E_f b} \tag{3.14}$$

where

$$\begin{aligned}\overline{v}(\xi) &= \Big[6f_\psi(\xi)\frac{C_{v\psi}^2}{C_{vv}C_\psi}\frac{1}{\lambda^2} - \frac{1}{2}(2\xi - \xi^2 - 1)\xi^2\Big]\frac{\lambda^3}{C_{vv}}\\ f_\psi(\xi) &= \xi - \xi^2 - \frac{\cosh(\alpha\lambda/2) - \cosh[(\alpha\lambda(1-2\xi)/2]}{\alpha\lambda\sinh(\alpha\lambda/2)}\end{aligned} \tag{3.15}$$

Consequently, the relative maximum deflection

$$\overline{v}_{max} = \overline{v}\Big(\frac{1}{2}\Big) = \overline{v}_{max}\frac{q}{E_f b} \tag{3.16}$$

where the dimensionless maximum deflection

$$\overline{v}_{max} = \overline{v}\Big(\frac{1}{2}\Big) = (1 + C_{se})\frac{\lambda}{32C_{vv}} \tag{3.17}$$

and the shear coefficient

$$C_{se} = 48\Big[1 - 4\frac{\cosh(\alpha\lambda/2)}{\alpha\lambda\sinh(\alpha\lambda/2)}\Big]\frac{C_{v\psi}^2}{C_{vv}C_\psi}\frac{1}{\lambda^2} \tag{3.18}$$

The shear stresses described by Eqs. (2.8), (2.9) and (2.10), with consideration of Eqs. (2.16), (2.17) and (2.18), in successive layers, are as follows:
— the upper face $(-1/2 \leqslant \eta \leqslant -\chi_c/2)$

$$\tau_{xy}^{(uf)}(x,\eta) = \overline{\tau}_{xy}^{(uf)}(x,\eta)\frac{q}{b} \tag{3.19}$$

where, the dimensionless stress

$$\overline{\tau}_{xy}^{(uf)}(x,\eta) = \frac{1}{2(1+\nu)}\overline{Q}_z^{(uf)}\overline{\psi}_f(x) \tag{3.20}$$

— the core $(-\chi_c/2 \leqslant \eta \leqslant \chi_c/2)$

$$\overline{\tau}_{xy}^{(c)}(x,\eta) = \frac{1}{2(1+\nu)}\overline{Q}_z^{(c)}\overline{\psi}_f(x) \tag{3.21}$$

— the lower face $(\chi_c/2 \leqslant \eta \leqslant 1/2)$

$$\overline{\tau}_{xy}^{(lf)}(x,\eta) = \frac{1}{2(1+\nu)}\overline{Q}_z^{(lf)}\overline{\psi}_f(x) \tag{3.22}$$

Exemplary calculations are carried out for a beam family of the following selected dimensionless sizes and material constants: $\lambda = 30$, $\chi_c = 4/5$, $e_c = 1/30$, $\nu = 0.3$, as well as the exponent – natural number $n = 0, 2, 7, 14, 25, \rightarrow \infty$. The graphs of the dimensionless functions given in Eqs. (2.2), (2.3) and (2.4) of Young's modulus variation and the dimensionless shear stresses in Eqs. (3.20), (3.21) and (3.22) in the beam cross section for $\xi = 0.1$, and the exponent value $n = 7, \rightarrow \infty$ are shown in Figs. 6a and 6b. The maximum shear stress $\overline{\tau}_{max}(\xi) = \overline{\tau}_{xy}^{(c)}(\xi, 0)$ occurs at the neutral surface $(\eta = 0)$ in the core.

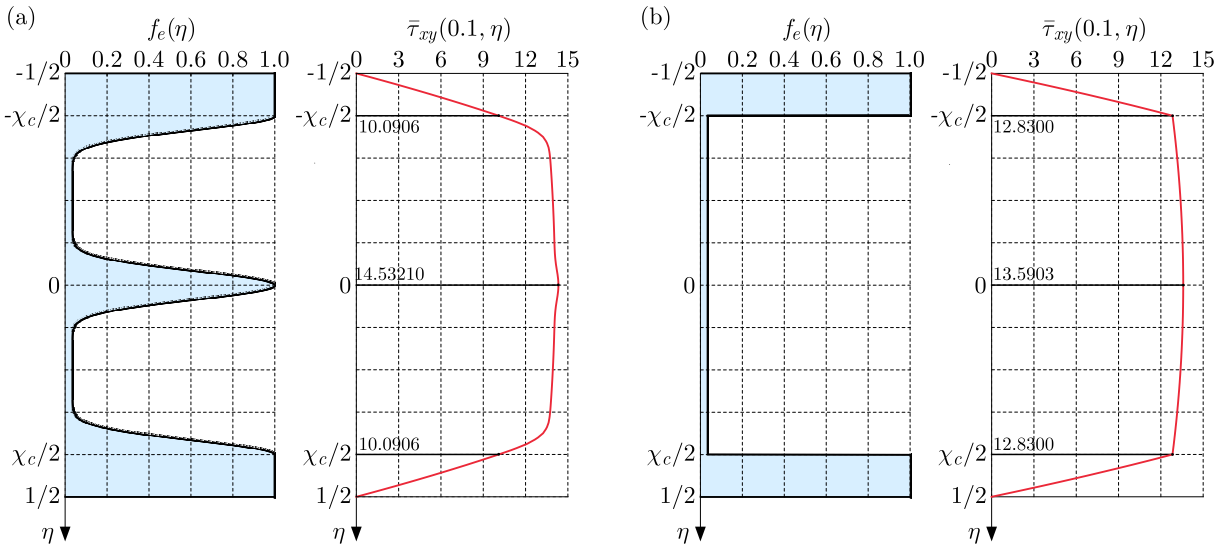

Fig. 6. The graph of dimensionless functions of Young's modulus variation and the dimensionless shear stress: (a) for $n = 7$ and (b) classical sandwich beam for $n \rightarrow \infty$

The results of analytical calculations of the dimensionless coefficient C_{vv}, maximum dimensionless shear stresses, shear coefficient C_{se}, Eq. (3.18), and dimensionless maximum deflection $\overline{v}_{max}$, Eq. (3.17), are specified in Table 1.

Table 1. The value of coefficients, shear stresses and maximum deflections – analytical calculations

	n					
	0	2	7	14	25	∞
C_{vv}	1.0	0.73063	0.64218	0.60630	0.58281	0.505067
$\overline{\tau}_{max}$	18.0000	15.1103	14.3210	14.0761	13.9253	13.5903
C_{se}	0.01376	0.09186	0.13953	0.15146	0.15996	0.17078
$\overline{v}_{max}$	855.4	1260.9	1497.2	1604.8	1679.4	1955.9

Moreover, the graphs of maximum dimensionless shear stresses $\overline{\tau}_{max}$ and maximum deflections $\overline{v}_{max}$ are shown in Figs. 7a and 7b.

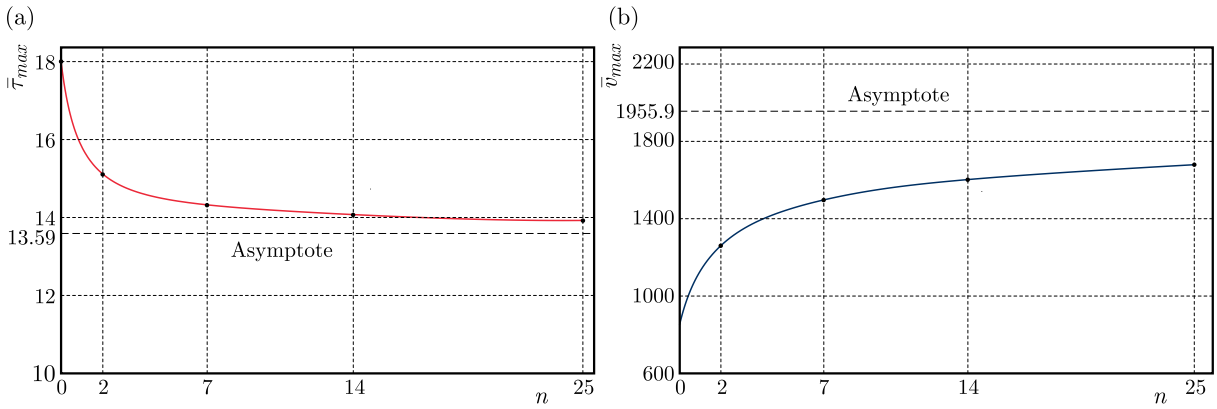

Fig. 7. The graph of (a) the maximum dimensionless shear stresses $\overline{\tau}_{max}$ and (b) the maximum dimensionless deflections $\overline{v}_{max}$

4. Numerical FEM bending study of the sandwich beam

The numerical model of the family of selected beams with the same parameters as in the analytical study is developed in the Ansys 2021 R2 system and is examinef in linear static structural analysis. The following parameters are applied in the study: $E_f = 70\,\text{GPa}$, $b = 50\,\text{mm}$, $h = 50\,\text{mm}$, thus $L = 1500\,\text{mm}$ ($\lambda = 1/30$).

Due to symmetry of the geometry, load and mechanical parameters, only a quarter of the beam is considered. The symmetric boundary conditions are applied by restricting the normal displacements at the selected faces shown in Fig. 8a. The clamped boundary condition is imposed on the face of the free end of the beam in the following manner. Displacements along the y-axis are blocked referring to the remote point located in the centre of the coordinate system ($v = 0$). In addition, the translations towards the x-axis are restrained globally ($u = 0$) on the same face. Such a boundary condition is consistent with analytical study and also allows deformations of the face at the end of the beam in the y and z directions, which ensures no stress concentration phenomenon. The force $F_y = 1\,\text{kN}$ is applied to the top of the quarter of the model, which corresponds to the uniformly distributed load (Fig. 1) of $q = 8/3\,\text{N/mm}$.

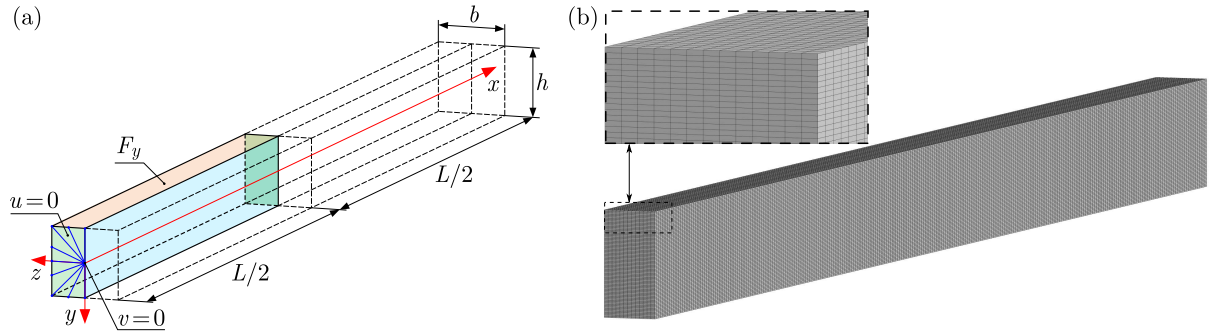

Fig. 8. (a) Geometry and boundary conditions in finite element analysis. (b) Numerical FEM model of the sandwich beam

The geometry is divided into uniform second-order hexahedral SOLID186 finite elements with twenty nodes and three degrees of freedom at each node (Fig. 8b). A sufficient number of finite elements is found through mesh convergence study with the accuracy criterion imposed on the maximum deflection, shear stress, and elastic strain energy. Such an analysis is carried out assuming the greatest gradient of Young's modulus except for $n \to \infty$, that is, for $n = 25$. The finite element model consists of over 1.3 million nodes and 312 thousand elements, assuming there are 300, 80 and 13 elements along x, y and z directions (Fig. 8a), respectively. The ratio

of the number of elements to the model size is highest along the depth of the beam (y-axis) due to the variable mechanical property towards this direction.

The mechanical properties of the material are coherent with analytical study, i.e. isotropic, perfectly elastic, where Young's modulus is described by the function in Eqs. (2.1) and (2.3). At any point of the geometry, the calculated values of Young's modulus are mapped to the centres of hexahedral finite elements. An exemplary distribution of Young's modulus for $n = 2$ is shown in Fig. 9.

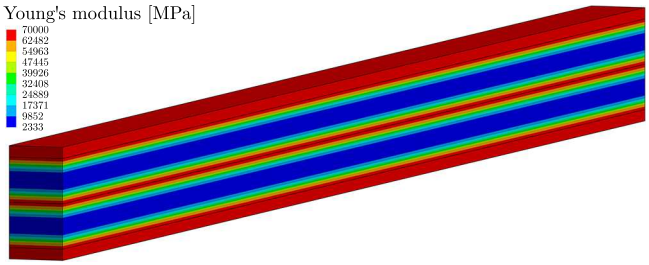

Fig. 9. Young's modulus E distribution for $n = 2$

The deflections v obtained for this case, i.e. displacements toward the y-axis, are shown in Fig. 10a. Following the analytical study, the shear stress is studied for $\xi = x/L = 0.1$. In that case, the surface at $x = 150\,\text{mm}$ parallel to the yz plane is considered as presented in Fig. 10b.

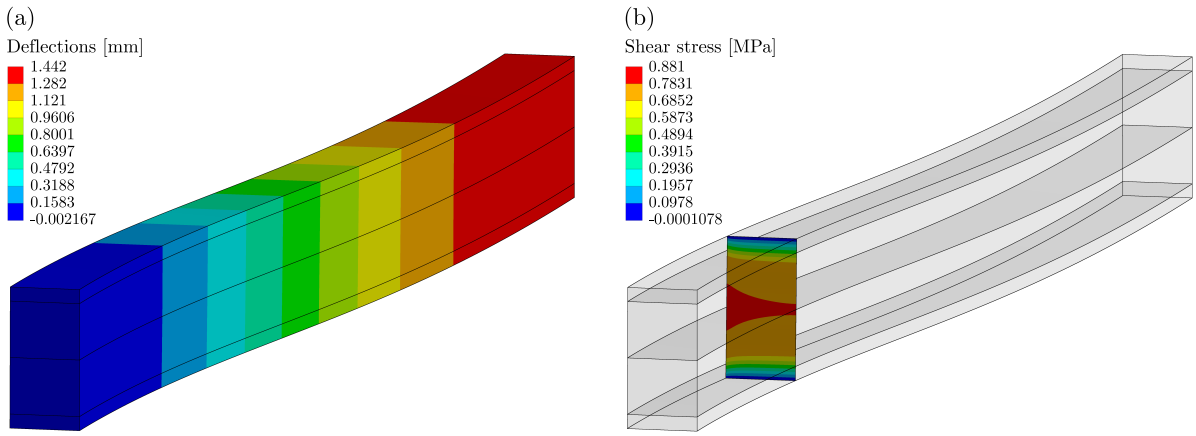

Fig. 10. (a) Deflections $v(x)$ for $n = 2$. (b) Shear stress τ_{xy} in the surface parallel to yz plane at $x = 150\,mm$ $(\xi = x/L = 0.1)$ for $n = 2$

The results of the numerical study are further compared with the analytical solutions. It should be noted that in the case of a three-dimensional finite element model, the shear stress τ_{xy} varies along the width of the beam (Fig. 10b). To study the results, the mean of that function along width is considered. The maximum deflection v_{max} in FEM analyses are taken from the neutral surface for $z = 0$. To maintain consistency with the analytical study, the obtained results are further considered in a dimensionless form, that is

$$\overline{v}_{max} = \frac{E_f b}{qL} v_{max} \qquad \overline{\tau}_{max} = \frac{b}{q} \tau_{max} \tag{4.1}$$

Exemplary distributions of shear stress along the depth of the beam described by the dimensionless parameter η and corresponding dimensionless functions of Young's modulus are presented in Figs. 11a and 11b. These show a near-perfect agreement with the analytical outcomes shown in Figs. 6a and 5b.

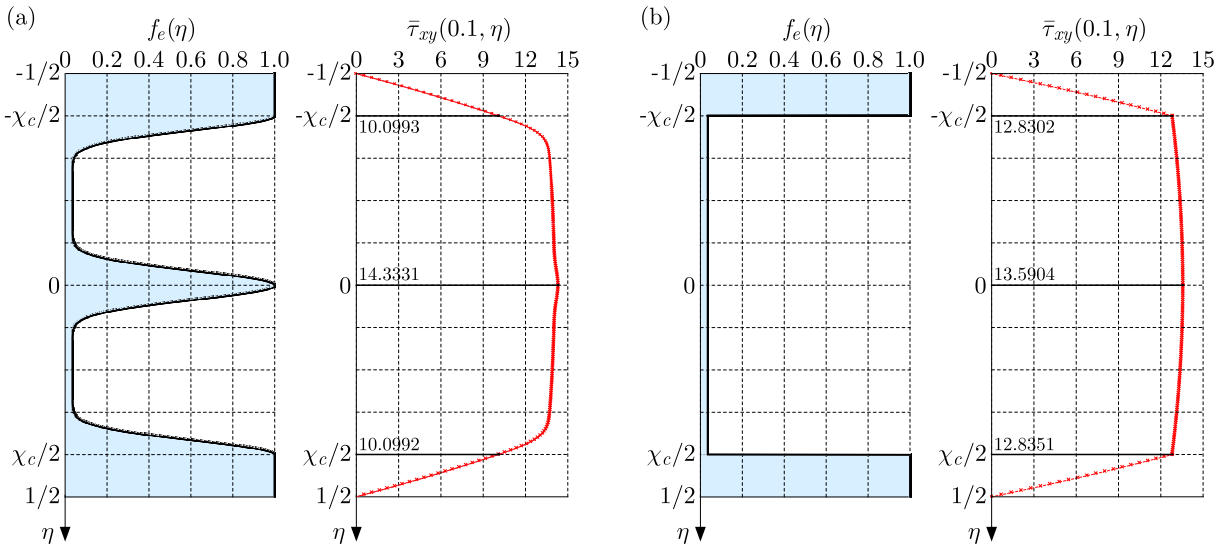

Fig. 11. The graph of dimensionless functions of Young's modulus variation and dimensionless shear stress (a) for $n = 7$ and (b) for $n \to \infty$ from the numerical study

The numerically obtained maxima of shear stress $\overline{\tau}_{max}$ and deflections $\overline{v}_{max}$ for all the values considered of the parameter n are summarised in Table 2 in a dimensionless form. When comparing the dimensionless maximum shear stresses and deflections calculated analytically and numerically (Tables 1 and 2), it is easy to notice that the differences between them are insignificant, less than 0.1%.

Table 2. The maximum shear stresses and deflections – numerical FEM analysis

	n					
	0	2	7	14	25	∞
$\overline{\tau}_{max}$	18.0023	15.1169	14.3331	14.0808	13.9379	13.5904
$\overline{v}_{max}$	854.9	1261.0	1497.7	1605.6	1680.4	1956.9

5. Conclusions

Most of the papers investigating the problem of the shear effect in beams refer to numerical methods or analytical studies, whereas the deformation function is assumed in advance within the number of theories mentioned in the literature review. The choice of the deformation function can have a direct effect on the accuracy of the solution. In the present paper, a linear theory with the assumption of nonlinear shear deformation is developed and applied taking into account the classical shear stress formula for beams. Unlike the number of theories and papers, the shear deformation function is the result of an analytical solution, which leads to an exceptionally coherent solution compared to the FEM study.

The generalised form of the function that describes Young's modulus allowed us to analyse beams with various mechanical properties, including homogeneous and layered beams within the proposed theory. Using the principle of stationary potential energy, two differential equations of equilibrium were derived and then solved. Relative deflections and shear stresses were calculated for exemplary beams with different variations in Young's modulus.

To verify the accuracy of the developed theory, the outcome of the analytical study was compared with the results of numerical FEM analysis in the Ansys system. The beam was

modelled as a three-layered structure, while its core had a variable Young's modulus along its depth.

Following the results in Figs. 6 and 12, both analytical and numerical analyses yielded consistent shear stress distributions for all exemplary structures. Comparison of the maximum relative deflection and maximum relative shear stress shown in Tables 1 and 2 shows a nearly identical result from both methods. The relative differences between these are less than 0.1%, proving that the theory developed is accurate. Having in mind the fact that it is suitable for beams with different Young's modulus distributions, i.e. homogenous and nonhomogeneous, it can be applied to numerous practical analyses of composite structures.

Acknowledgement

The paper is developed based on the scientific activity of the Łukasiewicz Research Network – Poznan Institute of Technology, Rail Vehicles Center, and the statutory activity of the Poznan University of Technology, funded by the Ministry of Science and Higher Education in Poland (grant No. 0612/SBAD/3605).

References

1. Banat D., Mania R.J., 2017, Failure assessment of thin-walled FML profiles during buckling and postbuckling response, *Composites Part B: Engineering*, **112**, 278-289
2. Berdichevsky V.L., 2010, An asymptotic theory of sandwich plates, *International Journal of Engineering Science*, **48**, 3, 383-404
3. Birman V., Kardomateas G.A., 2018, Review of current trends in research and applications of sandwich structures, *Composites Part B: Engineering*, **142**, 221-240
4. Carrera E., Giunta G., Petrolo M., 2011, *Beam Structures, Classical and Advanced Theories*, John Wiley & Sons
5. Dhuria M., Grover N., Goyal K., 2021, Influence of porosity distribution on static and buckling responses of porous functionally graded plates, *Structures*, **34**, 1458-1474
6. Domagalski Ł., Jędrysiak J., 2016, Geometrically nonlinear vibrations of slender meso-periodic beams. The tolerance modeling approach, *Composite Structures*, **136**, 270-277
7. Ghayesh M.H., 2018, Vibration analysis of shear-deformable AFG imperfect beams, *Composite Structures*, **200**, 910-920
8. Huang S.J., 2003, An analytical method for calculating the stress and strain in adhesive layers in sandwich beams, *Composite Structures*, **60**, 1, 105-114
9. Jędrysiak J., 2023, Theoretical tolerance modelling of dynamics and stability for axially functionally graded (AFG) beams, *Materials*, **16**, 5, 2096
10. Kolakowski Z., Mania R.J., 2015, Dynamic response of thin FG plates with a static unsymmetrical stable postbuckling path, *Thin-Walled Structures*, **86**, 10-17
11. Kumar R., Lal A., Singh B.N., Singh J., 2019, New transverse shear deformation theory for bending analysis of FGM plate under patch load, *Composite Structures*, **208**, 91-100
12. Magnucki K., 2022, An individual shear deformation theory of beams with consideration of the Zhuravsky shear stress formula, *Current Perspectives and New Directions in Mechanics, Modelling and Design of Structural Systems*, 682-689
13. Magnucki K., Lewinski J., Magnucka-Blandzi E., 2020, A shear deformation theory of beams of bisymmetrical cross sections based on the Zhuravsky shear stress formula, *Engineering Transactions*, **68**, 4, 353-370
14. Magnucki K., Magnucka-Blandzi E., Wittenbeck L., 2022, Bending of a generalized circular sandwich plate under a concentrated force with consideration of a nonlinear shear deformation theory, *Archives of Mechanics*, **74**, 267-282

15. Mahi A., Adda Bedia E.A., Tounsi A., 2015, A new hyperbolic shear deformation theory for bending and free vibration analysis of isotropic, functionally graded, sandwich and laminated composite plates, *Applied Mathematical Modelling*, **39**, 9, 2489-2508

16. Mantari J.L., Oktem A.S., Guedes Soares C., 2012, A new higher order shear deformation theory for sandwich and composite laminated plates, *Composites Part B: Engineering*, **43**, 3, 1489-1499

17. Marczak J., Jędrysiak J., 2015, Tolerance modelling of vibrations of periodic three-layered plates with inert core, *Composite Structures*, **134**, 854-861

18. Meiche N.E., Tounsi A., Ziane N., Mechab I., Adda Bedia E.A., 2011, A new hyperbolic shear deformation theory for buckling and vibration of functionally graded sandwich plate, *International Journal of Mechanical Sciences*, **53**, 4, 237-247

19. Özütok A., Madenci E., 2017, Static analysis of laminated composite beams based on higher-order shear deformation theory by using mixed-type finite element method, *International Journal of Mechanical Sciences*, **130**, 234-243

20. Pei Y.L., Geng P.S., Li L.X., 2018, A modified higher-order theory for FG beams, *European Journal of Mechanics – A/Solids*, **72**, 186-197

21. Reddy J.N., 2004, *Mechanics of Laminated Composite Plates and Shells: Theory and Analysis*, CRC Press

22. Sahoo R., Singh B.N., 2013, A new shear deformation theory for the static analysis of laminated composite and sandwich plates, *International Journal of Mechanical Sciences*, **75**, 324-336

23. Thai H.-T., Vo T.P., 2013, A new sinusoidal shear deformation theory for bending, buckling, and vibration of functionally graded plates, *Applied Mathematical Modelling*, **37**, 5, 3269-3281

24. Zenkour A.M., 2006, Generalized shear deformation theory for bending analysis of functionally graded plates, *Applied Mathematical Modelling*, **30**, 1, 67-84

25. Żur K.M., Arefi M., Kim J., Reddy J.N., 2020, Free vibration and buckling analyses of magneto-electro-elastic FGM nanoplates based on nonlocal modified higher-order sinusoidal shear deformation theory, *Composites Part B: Engineering*, **182**, 107601

Manuscript received August 3, 2023; accepted for print September 12, 2023